Photodeformation Behavior of Photodynamic Polymers Bearing Azobenzene Moieties in Their Main and/or Side Chain

Chang-Dae Keum, Taiji Ikawa, Masaaki Tsuchimori, and Osamu Watanabe*

Toyota Central Research and Development Laboratories Inc., 41-1 Yokomichi, Nagakute, Nagakute-cho, Aichi 480-1192, Japan

Received January 29, 2003; Revised Manuscript Received March 25, 2003

ABSTRACT: This paper describes a comparative study of polymers containing push−pull type azobenzene moieties in their main and/or side chains. The polymers were systematically designed and synthesized specifically for this work in order to investigate their photodeformation through the migration of polymer chains, which was induced by an optical field generated around some polystyrene (PS) spheres. The PS spheres, which had a diameter of 990 nm, were arranged on the surface of the photodynamic polymer films by a self-organization process, and the films were then exposed to a linearly polarized Kr−Ar laser at 488 nm. Although the azobenzene moieties in the polymers exhibited a remarkably slow trans−cis−trans isomerization cycle, a series of hexagonally arrayed indented structures that reflected the geometry and arrangement of the spheres were successfully observed using atomic force microscopy (AFM). The depths of these dents were consistent with the dynamics of the azobenzene moiety in the polymers. The molecular weight, glass transition temperature (T_g), and absorptivity at the wavelength of the irradiating light were nearly identical for all of the materials that we used. However, the total amount of mass transport that occurred on the polymer surfaces did not depend directly on the efficiency of the photoisomerization, which was more related to the structure (i.e., main- or side-chain type) of the polymers. Furthermore, analysis of the polymer migration using tapping mode atomic force microscopy (TMAFM) revealed that the mechanism of the mass transport was clearly between the main- and the side-chain type polymers, which may be due to differences in the migration mechanism of the polymer chain.

Introduction

Azobenzene-containing polymers have drawn considerable attention in the past few decades, mainly based on the two different configurations (trans and cis forms) of the azobenzene derivatives.[1−21] These two forms can isomerize reversibly by photo- or thermochemical processes, leading to a drastic change in the physical and optical properties of the materials. This property provides enormous potential for the materials to be used in the fields of photonics and optical information storage.[1−5] In particular, recent studies of the fabrication of surface relief structures in such polymer films by exposure to an interference light pattern or a single-laser beam show their potential for new surface modification processes, e.g., photolithography and surface relief gratings. The mechanism that leads to the surface relief structure of these materials, which is based on a photoinduced mass transport process of the polymer chains, has already been reported.[6−8]

Near-field optics are currently being extensively investigated from the viewpoint of nanoscale optical science and technology for superfine photolithography and high-density optical data.[9,10] This is because the modification size of a conventional light source is restricted by the diffraction limit of the exposed light. We recently reported a topographical change on the surface of azobenzene functionalized polymer films that was induced by means of an optical near field generated around polystyrene (PS) spheres of submicron diameter.[11] The indented structure that we formed was thermally stable and could be erased by heating the polymer film above its T_g. Moreover, we have also succeeded in transcribing a monolayer of 28 nm diameter spheres into a topographic image on an azobenzene polymer surface.[11a] More recently, the mechanism for the surface deformation induced on the surface of the polymer that we achieved in our work using the PS spheres has also been reported.[11e]

To realize the finely tuned modification of the surface of a polymer film, its chemical structure should be designed on the basis of a fully elucidated understanding of the photodeformation process. We have explored the surface modification of a thin film of polyurethanes, each containing a slightly different azobenzene moiety in the side chain, with the aim of achieving a finely tuned surface modification.[11f] Polymers only containing the azobenzene moiety in their side chain were studied in our previous work. Azobenzene groups can also be incorporated into the main chain of polymers,[12−20] and photomechanical and nonlinear optical (NLO) effects in various main-chain azo polymers have been previously reported.[15−19] Lee et al. recently reported photoinduced dichroism, birefringence, and surface profile gratings in high-T_g polyureas with mono- or bis-azoaromatic groups in the main chain.[17] More recently, birefringence and surface profile gratings have also been studied in amorphous polyesters with amino-sulfone azobenzene chromophores in the main chain.[20]

In this article, polymers containing push−pull type azobenzene in the side and/or main chains are reported. The polymers were systematically designed and synthesized to explore their deformation behavior on the basis of the azobenzene groups incorporated into their side or main chains. We investigated their photoisomerization behavior and surface modification properties in order to understand and evaluate the photodeformation of the polymer thin films. Furthermore, we determined the total amount of mass transport that took place on the azobenzene polymer surface as well as performing TMAFM to elucidate the nature of the photodeforma-

* To whom correspondence should be addressed: phone +81-561-63-6169; Fax +81-561-63-6137; e-mail e0909@mosk.tytlabs.co.jp.

10.1021/ma034122y CCC: $25.00
Published on Web 06/05/2003

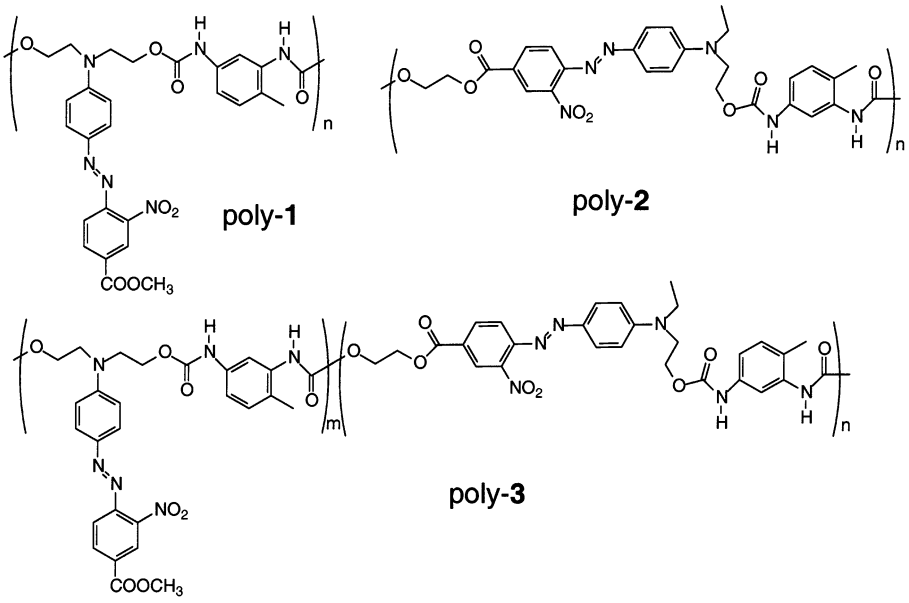

Figure 1. Chemical structures of the azobenzene-containing polymers used in this study.

Scheme 1. Synthetic Routes for Azobenzene Monomers, M1 and M2

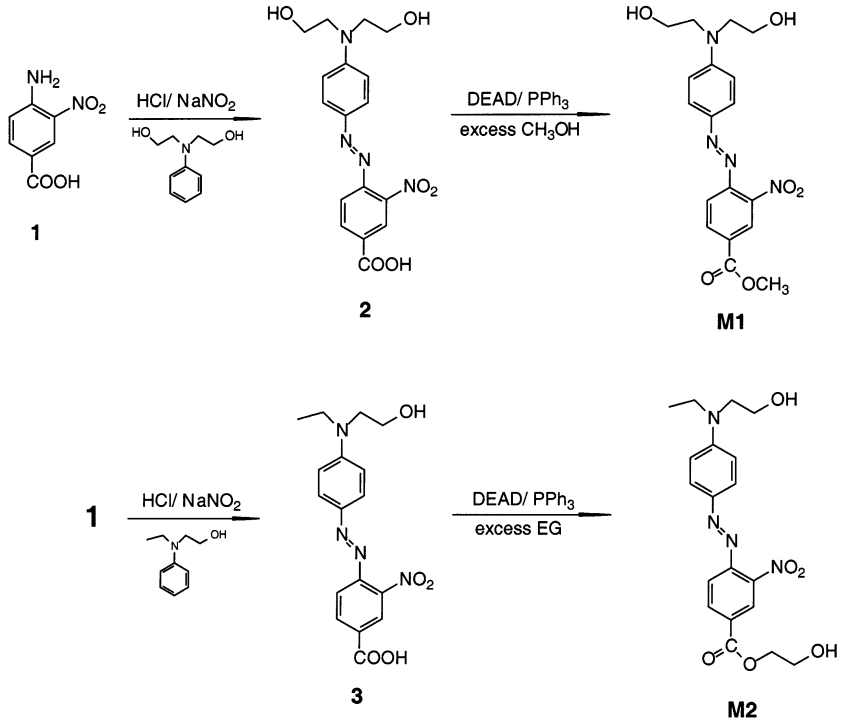

tion. A possible mechanism for the behavior that we observed is also discussed.

Experimental Section

This investigation was performed using poly-**1**, poly-**2**, and poly-**3**, whose structures are shown in Figure 1. The synthetic routes for **M1** and **M2** and their polymerization with 1,3-TDI are outlined in Schemes 1 and 2, respectively. **M1** and **M2** were synthesized using a procedure similar to that in the literature.[19]

Materials. Triphenylphosphine (PPh_3), 3-nitro-4-aminobenzoic acid, and ethylene glycol from Wako Pure Chemical Industries, Ltd., were used as received without further purification. Diethanolaniline, *N*-ethyl-*N*-(hydroxyethyl)aniline, and diethylazodicarboxylate (DEAD) from Aldrich Chemical Co. were also used without further purification. Tetrahydrofuran (THF), dimethylformamide (DMF), and all other reagents were also used as received.

Synthesis. 2-Nitro-4-carboxy-4′-[*N*,*N*-di(2-hydroxyethyl)-amino]azobenzene (2) (Scheme 1). A solution of 56 mL of hydrochloric acid (5 mol L^{-1}) was cooled to 0 °C, and sodium nitrate (0.53 g, 7.71 mmol) in 7 mL of water was slowly added. 3-Nitro-4-aminobenzoic acid (1) (7.0 g, 38.5 mmol) was dissolved in a solution of sodium hydroxide (1.54 g, 38.5 mmol) in 58 mL of water and was then combined with a solution of sodium nitrate (2.80 g, 40.58 mmol) in 18 mL of water. This solution was slowly added under stirring to the hydrochloric acid solution while the temperature was kept within 5−10 °C. At the end of the diazotization, a fine precipitate of the diazonium salt was formed. After complete addition, the solution was allowed to stir for another 30 min, and a spatula of urea was then added to destroy any excess sodium nitrate. The prepared diazonium solution was then added to a solution of diethanolaniline (7.0 g, 38.5 mmol) in 70 mL of ethanol at 5−10 °C. The clear solution immediately turned red, and a precipitate was formed after a short time. After complete

Scheme 2. Synthetic Routes for Azobenzene-Containing Polymers Used in This Study

Table 1. Molecular Weight and Glass Transition Temperature of the Azobenzene Polymers Used in This Work

polymer	M_n[a]	M_w/M_n[a]	T_g (°C)[b]
poly-**1**	7200	1.7	134
poly-**2**	4300	1.3	112
poly-**3**	6500	1.4	125

[a] Determined by GPC using a polystyrene-calibrated column set. [b] Determined from DSC measurements.

addition, the mixture was stirred for another 30−40 min, and then sodium acetate (3.0 g) and sodium chloride (6.0 g) in 100 mL of water were added. The precipitate was filtered off, washed with water, and carefully dried under vacuum. The resulting compound, which was nearly black in color, was recrystallized twice from toluene. Yield: 8.2 g (57%).

2-Nitro-4-methylcarboxylate-4′-[*N,N*-di(2-hydroxyethyl)-amino]azobenzene (M1) (Scheme 1). PPh_3 (5.24 g, 20 mmol) was added all at once to a stirred solution of DEAD (3.48 g, 20 mmol), **2** (7.5 g, 20 mmol), and methanol (12.8 g, 0.4 mol) in dry THF (40 mL). The reaction mixture was stirred for 12 h, and the solvent was evaporated under vacuum. The remaining product was purified by column chromatography (silica gel, chloroform/EtOAc as eluent). Yield: 6.8 g (87%). ^{1}H NMR ($CDCl_3$): 8.48 (d, 1H, *CH* in aromatic), 8.23 (m, 1H, *CH* in aromatic), 7.83 (d, 2H, *CH* in aromatic), 7.72 (d, 1H, *CH* in aromatic), 6.77 (d, 2H, *CH* in aromatic), 3.96 (s, 3H, $-COOCH_3$), 3.94 (t, 4H, $-CH_2CH_2OH$), 3.73 (t, 4H, $-CH_2-CH_2OH$).

2-Nitro-4-carboxy-4′-[*N*-(hydroxyethyl)-*N*-ethylamino]-azobenzene (3) (Scheme 1). The above procedure for compound **2** was repeated using 3-nitro-4-aminobenzoic acid (**1**) (7.0 g, 38.5 mmol) and *N*-ethyl-*N*-(hydroxyethyl)aniline (6.4 g, 38.5 mmol) in 70 mL of ethanol.

The product, which again was a nearly black compound, was recrystallized twice from toluene. Yield: 6.9 g (50%).

2-Nitro-4-hydroxyethylcarboxylate-4′-[*N*-(hydroxyethyl)-*N*-ethylamino]azobenzene (M2) (Scheme 1). The above procedure for compound M1 was repeated using 3 (1.8 g, 4.9 mmol) and excess ethylene glycol (3.0 g, 49 mmol). The resulting product was collected by filtration and purified by column chromatography (silica gel, chloroform/EtOAc as eluent) to give M2. Yield: 1.7 g (87%). ^{1}H NMR ($CDCl_3$): 8.51 (s, 1H, *CH* in aromatic), 8.28 (d, 1H, *CH* in aromatic), 7.90 (d, 2H, *CH* in aromatic), 7.77 (d, 1H, *CH* in aromatic), 6.91 (d, 2H, *CH* in aromatic), 4.53 (t, 2H, $-COOCH_2CH_2OH$), 4.01 (t, 2H, $-COOCH_2CH_2OH$), 3.90 (t, 2H, $-CH_2CH_2OH$), 3.64 (t, 2H, $-CH_2CH_2OH$), 3.56−3.61 (m, 2H, $-CH_2CH_3$), 1.27 (t, 3H, $-CH_2CH_3$).

Polymerization. The procedure for poly-**1** in Table 1 is described as a typical example. A solution of **M1** (0.24 g, 0.59 mmol) in DMF (4 mL) was added slowly to a solution of 2,4-TDI (0.087 mL, 0.61 mmol) in DMF (0.3 mL). The reaction was performed for 24 h at 100 °C before the addition of dibutyltin dilaurate (ca. 0.5 wt %). The reaction then continued for another 36 h before the addition of methanol to quench the reaction. The solution was added slowly to methanol to precipitate the polymer. The final product was obtained by drying at 70 °C for 24 h, yielding 0.27 g (78%) of a dark red powder.

Table 2. UV−Vis Absorption Maxima of Azo Monomers and Polymers Used in This Work in DMF Solution and in Films at Room Temperature

		λ_{max} (nm)	
	sample	in DMF	in film
monomer	**M1**	504	
	M2	504	
polymer	poly-**1**[a]	484	474
	poly-**2**[b]	494	488
	poly-**3**[c]	491	482

[a] Containing an azobenzene moiety only in the side chain. [b] Containing an azobenzene moiety only in the main chain. [c] Containing azobenzene moieties with the same content in the main chain and the side.

Film Preparation. Samples were prepared as follows for optical measurement experiments and for photodeformation experiments. A polymer−DMF solution (ca. 2 or 20 wt %) was spin-coated onto a glass slide after filtration with a Teflon membrane filter (Millipore, 0.22 μm). The films that were obtained were placed in a vacuum oven at 130 °C for over 48 h to obtain solvent-free samples. The thickness of the polymer films was measured using a surface profiler (a subsidiary of Veeco Instruments Inc. Dektak3 ST).

Characterization and Optical Testing. All of the proton (^{1}H) NMR spectra were recorded on a Bruker 500 MHz spectrometer with the appropriate solvents (i.e., chloroform-*d* or DMSO-d_6) as an internal standard. The UV−vis spectra were measured on a Shimadzu UV2100 ultraviolet−visible spectrophotometer, either in a DMF solution or as a film. All of the differential scanning calorimetry (DSC) thermograms were obtained using a Perkin-Elmer DSC-7 and a TAC 7/DX thermal controller under a nitrogen atmosphere and a heating and cooling rate of 10 °C/min. The number- and weight-average molecular weights (M_n and M_w) of the polymers were measured by gel permeation chromatography (GPC) using a liquid chromatograph (Shimadzu LC-7A) with a column (Shodex KF-807L × 2) on NMP as an eluent, which was calibrated with standard polystyrene. The general properties of these polymers are summarized in Tables 1 and 2.

The optical measurements were performed using an unpolarized probe light, where the light beam was produced from a xenon lamp included within a monochromator (JASCO, SM-5). The beam was transmitted through the sample and was then fed to a detection system in which probe lights that were both parallel and perpendicular to the pump beam could be detected. For the pump beam itself, we used a linearly polarized Kr−Ar laser (Omnichrome, 643-AP) operating at a wavelength of 488 nm. The intensity of the pump beam was about 150 mW/cm^2. All of the measurements were performed at room temperature. An incident angle of 10° was employed for the pump beam with p-polarized incident light. In this work, the data obtained were analyzed without any consideration of the reflection from the surface and the interface of the sample film.

Surface Modification and Analysis. Photoinduced surface modification of the polymer films was performed by the following procedure. An aqueous solution including PS spheres (Moritex Co.) was dropped on the surface of the polymer films, and then the spheres were arranged by a self-organization process. After drying the samples at room temperature overnight, they were irradiated with a linearly polarized Kr−Ar laser at 488 nm (Omnichrome, 643-AP). The light irradiated the surface of the polymer films at normal incidence. The sample films were washed with water and benzene in order to remove the spheres from their surfaces and were subsequently dried in vacuo at room temperature for 2 days.

The surface structure on the polymer films was investigated under ambient conditions by contact mode AFM (Digital Instruments Inc., Nanoscope E). For all measurements, a 20 μm scanner was used in contact mode with a microlever force constant of 0.38 N/m. A scan rate of 2 Hz was employed.

TMAFM (Digital Instruments Inc., Nanoscope IIIa) was also performed to analyze the mass transport on the azobenzene

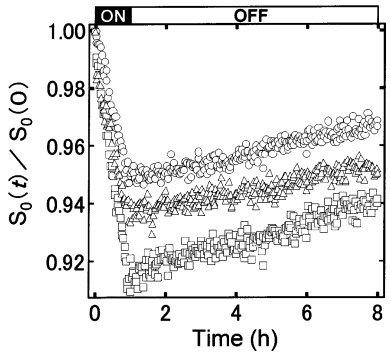

Figure 2. Changes in the average absorbance coefficient, $S_0(t)/S_0(0)$, during and after the exposure for poly-**1** (open squares), poly-**2** (open circles), and poly-**3** (open triangles). All of the samples were irradiated with 488 nm laser light at 150 mW/cm^2.

polymer surfaces. For the TMAFM, a commercial silicon cantilever (Nanosensor, SSS NCH8) was used. The radius of curvature of the tip was about 5 nm, the cantilever length was 125 μm, the contact force was 50 N/m, and the free resonant frequency was 298 kHz.

Results and Discussion

The maximum absorption wavelengths (λ_{max}) of the monomers, **M1** and **M2,** were almost the same in DMF solution (Table 2). However, the λ_{max} of the monomers after polymerization shifted to shorter wavelengths (blue shift). Furthermore, the λ_{max} of the polymers when they were cast into films shifted to still shorter wavelengths than they exhibited in solution, as shown in Table 2. It should be noted from the table that an azobenzene group in a side-chain type polymer (i.e., poly-**1**) gave a shorter λ_{max} than that of a main-chain type polymer (i.e., poly-**2**) in a film as well as in solution. On the other hand, poly-**3,** which has equal amounts of the azobenzene moiety in its main chain and in its side chain, had a λ_{max} intermediate between those exhibited by poly-**1** and poly-**2**. These results obviously indicate that the λ_{max} of the azo group was affected by the position of the azobenzene group in the polymers. In other words, the manner in which the group was attached (i.e., main or side chain) led to a change in the electronic environment of the azobenzene moiety, probably due to a difference in the association behavior of the neighboring azo dipoles in the main and side chains.

To investigate the photoisomerization behavior of the azobenzene groups in our polymers, we examined their average absorbance coefficient, $S_0(t)$, and dichroism, $S_2(t)$, during and after irradiation using linearly polarized light at 488 nm as a pump light (Figures 2 and 3). The (t) means specific time after turning on the pumping light. The $S_0(t)$ and $S_2(t)$ were studied using an unpolarized probe light at the appropriate λ_{max} (i.e., 474, 488, and 482 nm) for each of the polymer films and were obtained from the following relationships:

$$S_0(t) = (\alpha_{\parallel}(t) + 2\alpha_{\perp}(t))/3 \quad (1)$$

$$S_2(t) = \alpha_{\perp}(t) - \alpha_{\parallel}(t) \quad (2)$$

where $\alpha_{\parallel}(t)$ and $\alpha_{\perp}(t)$ are the absorbance coefficients, in the directions parallel and perpendicular to the polarization direction of the pump beam, respectively. The absorbance at around λ_{max} corresponds to the absorption by the trans isomer of the azobenzene moiety before irradiation. On the other hand, the absorption peaks

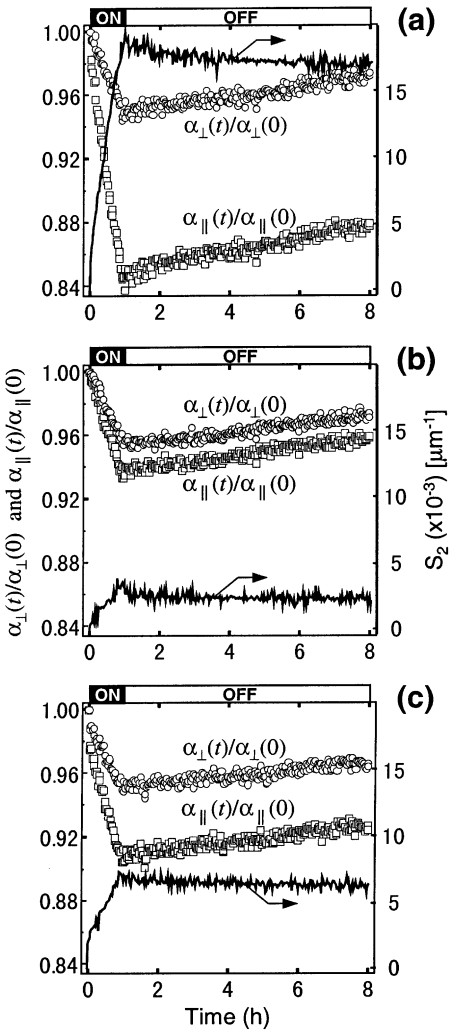

Figure 3. Changes in the dichroism, $S_2(t)$, and the normalized absorbance coefficients, $\alpha_{\parallel}(t)/\alpha_{\parallel}(0)$ (open squares) and $\alpha_{\perp}(t)/\alpha_{\perp}(0)$ (open circles), for films of (a) poly-**1**, (b) poly-**2**, and (c) poly-**3** during and after exposure. These samples were identical to those shown in Figure 2.

during and after irradiation are composed of absorptions due to both the trans and cis isomers.

On turning the pumping light on, the normalized $S_0(t)$ values ($S_0(t)/S_0(0)$) for each of the polymers decreased linearly and maintained this decrease during irradiation for 60 min without any saturation (Figure 2). On the other hand, the dichroism values $S_2(t)$ increased linearly during excitation (Figure 3). The changes in $S_0(t)/S_0(0)$ and $S_2(t)$ clearly depended on the structure of the polymers: the side-chain type polymer (poly-**1**) showed the most pronounced change, whereas the main-chain type polymer (poly-**2**) gave the slowest change. As we expected, the value of poly-**3**, containing the azobenzene groups in its main as well as its side chains, was between those of poly-**1** and poly-**2**. These results tell us that trans−cis isomerization of an azobenzene moiety due to covalent bonding in the main chain is more restricted than it is in a side chain.[17,20] After the pump light was turned off, the $S_0(t)/S_0(0)$ values recovered very slowly, 0.01−0.02 [h^{-1}], for all of the polymers. The recovery originating from the cis−trans thermal isomerization is clearly slower than the trans−cis photoisomerization. In the cis−trans isomerization process, ∼30% of the cis form of the polymer is isomerized to the trans form within 7 h of turning the light off. It

should be mentioned here that the photoisomerization rate of our polymers is obviously slower than that of common polymers containing push−pull type azobenzene (e.g., DR19).[22]

In these polymers, at least three factors that could lead to dichroism need to be considered. The first is the photobleaching of trans molecules by irradiation with polarized light, and the second is the reorientation of trans molecules during the continuous isomerization cycle and the rotational diffusion of the azo moiety. Finally, there is the stability of cis molecules, with very little reorientation to trans molecules, due to the restricted trans−cis−trans isomerization cycle.

As can be seen in Figure 2, our samples exhibited an increasing $S_0(t)/S_0(0)$ value after the light was turned off. After annealing at around their T_g of the photoirradiated sample, the changed $S_0(t)$ or $S_2(t)$ returned to former states, 1 or 0, respectively. These results strongly indicates that the dichroism is not caused by the first of the factors mentioned above, i.e., photobleaching, but is caused by the photinduced orientation or the trans−cis isomerization. The normalized $\alpha_\perp(t)/\alpha_\perp(0)$ and $\alpha_\parallel(t)/\alpha_\parallel(0)$ decrease continuously without any recovery in all of the polymers when the light is turned on, as seen in Figure 3. If the second factor occurred to any extent during the photoirradiation, the normalized $\alpha_\perp(t)/\alpha_\perp(0)$ should show an increase (after a temporary decrease when the light was turned on) due to the reorientation of trans molecules during the continuous isomerization cycle as well as the rotational diffusion of the azobenzene moiety. The results show that at least little in-plane orientation occurs. From our point of view, out-of plane orientation also has not any advantage to the in-plane orientation. Therefore, it can be considered that the possibility of in- or out-of-plane photoreorientation in the polymer is very low. From both the decrease of the $\alpha_\perp(t)/\alpha_\perp(0)$ and the $\alpha_\parallel(t)/\alpha_\parallel(0)$, we suppose that the dichroism may originate from the third factor, i.e., stable cis molecules. Namely, the dichroism in the polymers is mainly achieved through their trans−cis photoisomerization. The linear decreasing of $S_0(t)$ during irradiation for 1 h and the slow recovery of after turning off the pumping light, as shown in Figure 2, indicate that the lifetime of the cis isomer is quite long. The stability of the *cis*-azobenzene may be due to the intrinsic structure of the azobenzene with the nitro group in the ortho position. The structure of the azobenzene moiety with a nitro group in its ortho position may lead to a significantly diminished trans−cis−trans isomerization rate due to the steric hindrance of the nitro group during photoirradiation.

Next, we used an AFM to investigate the surface profile of polymer films (ca. 500 nm thickness). The films covered with 990 nm diameter PS spheres was irradiated for 60 min with a linearly polarized 488 nm wavelength Kr−Ar laser, and then the spheres were removed before observation. Figure 4 shows some typical examples of three-dimensional views of the film surfaces of the azobenzene polymers. The surfaces of the films prior to irradiation with the Kr−Ar laser showed no regular structural periodicity. Furthermore, it was observed that their surfaces were acceptably smooth. We also confirmed that the surface of the samples did not show any dents after the process without irradiation. After irradiation and removal of the spheres, it could be observed that hexagonally arrayed dents were formed on the surfaces of the polymer films,

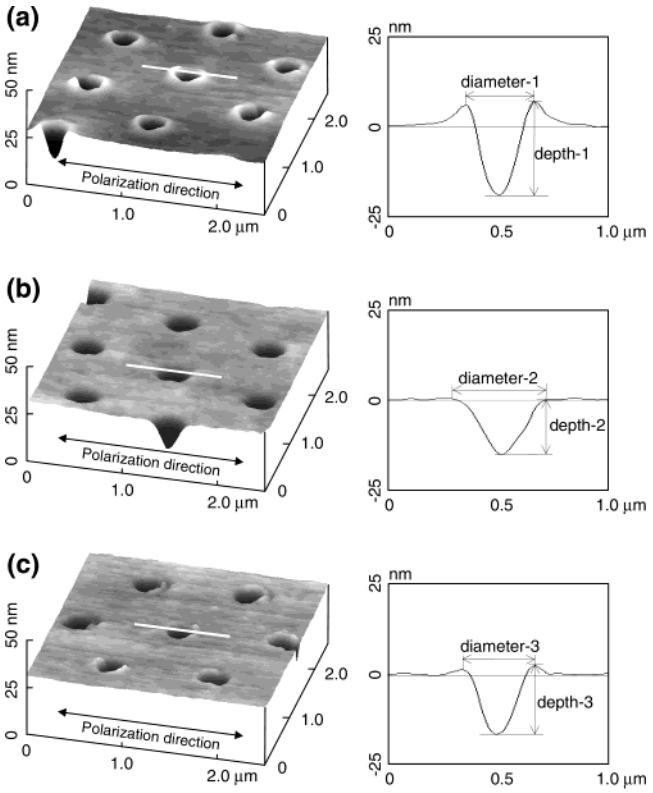

Figure 4. AFM three-dimensional view of the indented structure formed with PS spheres of 990 nm diameter on films of (a) poly-**1**, (b) poly-**2**, and (c) poly-**3**. All of the samples were irradiated with 488 nm laser light at 150 mW/cm^2 for 1 h.

despite the slow trans−cis−trans photoisomerization of their azobenzene groups. In our previous work we confirmed by scanning electron microscopy (SEM) that the dents are formed immediately below the PS spheres.[11c]

Therefore, it is reasonable to consider that the indented structures observed on the polymer films reflect the shape and arrangement of the spheres placed on the film's surface. The diameters (i.e., diameter-1, -2, and -3) of the dents induced on the polymer films were ca. 350−450 nm. The diameters of the dents obtained were clearly smaller than that of the spheres that we used. This result is considered to be brought about because the spheres act as lenses. On the other hand, a relatively large difference was observed in the depths (depth-1, -2, and -3) of the dents between the different polymers, although they have almost the same azo-dye content (i.e., ∼50 wt %). The depths of the dents in poly-**1**, poly-**2**, and poly-**3** were ∼25, ∼10, and ∼20 nm, respectively.

It should be noted here that the shape of the dents that were formed is clearly different. For the side-chain-type polymer (poly-**1**), the periphery of the dent formed a large hump in the polarization direction of the irradiation light (Figure 4a), and the main- and side-chain-type polymer (poly-**3**) showed a relatively smaller hump than that observed for poly-**1** (Figure 4c). Interestingly, no anisotropic hump could be seen on the main-chain-type polymer (poly-**2**) (Figure 4b). We also confirmed with very good reproducibility that the respective phenomena were independent of the irradiation time for all of the samples. The hump structure was only observed for polymers (i.e., poly-**1** and poly-**3**) with an azobenzene moiety in their side chain. These differences probably result from the different mass transport

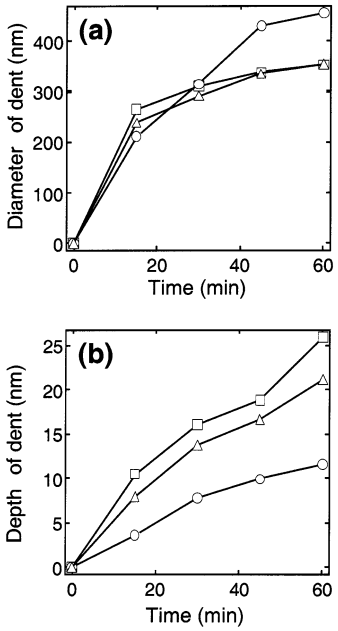

Figure 5. Changes in the sizes of the dents after the exposure: (a) diameter; (b) depth. The marks are identical to those shown in Figure 2. All of the samples were irradiated with 488 nm laser light at 150 mW/cm^2.

regimes of the polymer chains during the formation of the dents, which depend on the structure of the polymers. Namely, the results are related to the position (i.e., main or side chain) of the azobenzene group.

Figure 5 shows the effect of the irradiation time on the modification diameter and depth of the dents formed on the polymer films (ca. 500 nm thickness). The definition of the parameters (i.e., diameter and depth) is identical to that indicated in Figure 4. As shown in Figure 5a, the diameter of the dents formed on poly-**1** (□) was very similar to that of poly-**3** (△), which increased dramatically with increasing irradiation time up to 15 min, after which the increase became slower. For poly-**2** (○), the value increased linearly without any saturation, at least up to about 45 min.

On the other hand, the depth of the dents increased with increasing irradiation time without any saturation for at least 60 min for all of the polymers (Figure 5b). The depth of the dents on the film of poly-**1** had the largest value compared to those of the other polymers, and poly-**2** had the smallest value for all irradiation times. It is well-known that photoisomerization of the azobenzene moiety in a polymer clearly enhances the mobility of the material.[21] On the other hand, the mobility of the azo groups on the main chain in our polymers is restricted, and thus the orientation and relaxation can be hindered as mentioned above. Therefore, the difference in the depth of the dents on the polymers that we tested is probably due to differences in their mass transport properties depending on the efficiency of the softening by photoisomerization of the azobenzene groups. However, the shapes of dents on the poly-**2** film, which do not have any hump in the structure, are different from those of the other polymers, poly-**1** and poly-**3**. Therefore, to directly compare the amount of mass transport that take place for the different polymers, another parameter is needed.

For the purpose of comparing the surface photodeformation in the polymers, we used AFM data to determine the total amount of mass transport (V_M)

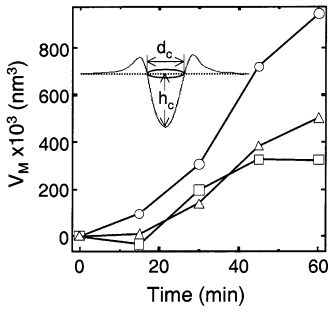

Figure 6. Total mass transport, V_M, of the polymers during the exposure. The marks are identical with those shown in Figure 2. All of the samples were irradiated with 488 nm laser light at 150 mW/cm^2 for 1 h. (Inset) Schematic illustration showing the definitions of d_c and h_c for the evaluation of V_M.

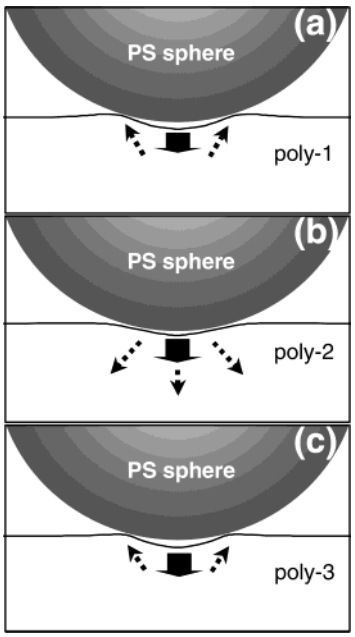

Figure 7. Migration of the polymer chains in the azobenzene polymers: (a) side-chain-type polymer, poly-**1**; (b) main-chain-type polymer, poly-**2**; (c) main- and side-chain-type polymer, poly-**3**. The movements of the polymer chains are represented in the images by the dotted arrows, and the solid arrows show the scattering force around the spheres induced by the optical electromagnetic field.

caused by the irradiation (Figure 6). V_M was calculated using the diameter, d_c, and height, h_c, of the pseudo-parabolic shaped dents that were formed and which are shown in the inset of Figure 6. As shown in the inset, d_c is the base diameter of the pseudo-parabolic shaped dents on the surface of the polymer films, and h_c is the distance between the vertex of the pseudo-parabolic dent and its base. Here, the curvature of the pseudo-parabolic dents was assumed to be the same for all of the polymers to simplify the calculation. The value V_M quantified the volume of a pseudo-parabolic shaped dent of diameter d_c and height h_c. This value is considered to be the sum of two different processes of mass transport during the photoirradiation. The first of these is the movement of the polymer chain from the center to the periphery, thereby forming the hump around the dent, and the second is the transportation from the polymer surface toward the substrate. The first process may be mainly assigned to the side-chain-type polymer, poly-**1**, with the humped structure in the periphery of the dent that is formed (Figure 7a). On the other hand, the second process may be the principal mass transport mechanism

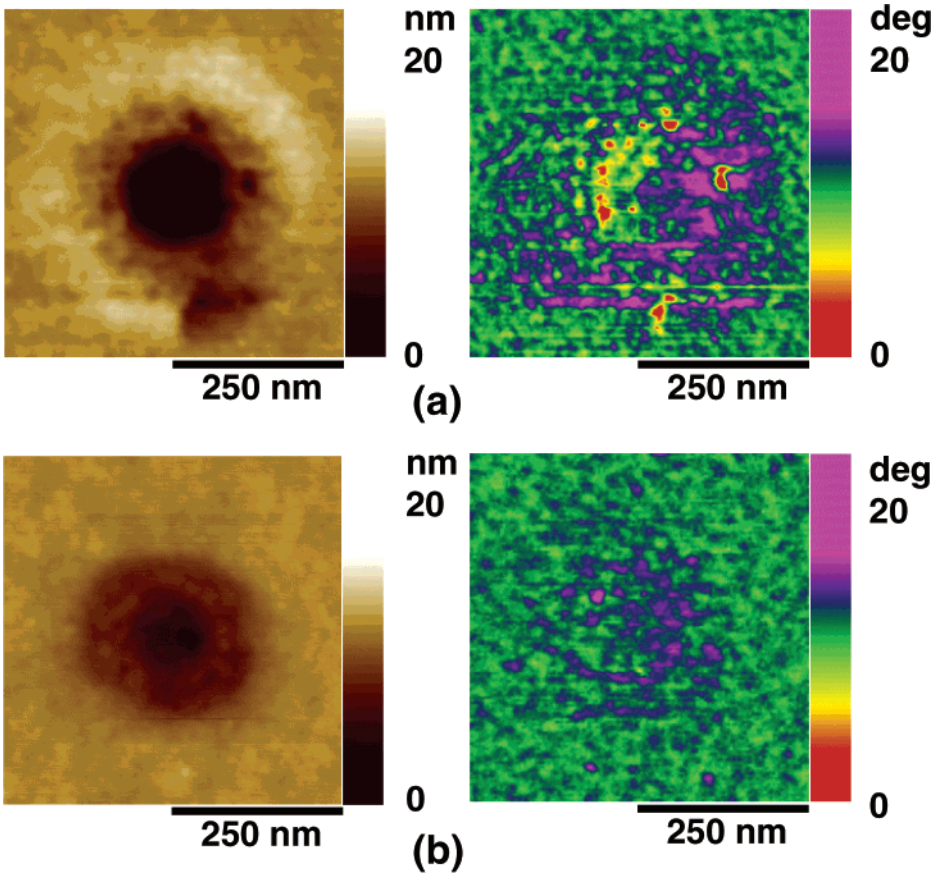

Figure 8. TMAFM images of the surface of the polymer films after the exposure: (a) poly-**1**; (b) poly-**2**. These samples were treated with the 990 nm spheres. The left-hand and right-hand images show the topographic and phase images, respectively. All of the samples were irradiated with 488 nm laser light at 150 mW/cm^2 for 1 h.

for the main-chain-type polymer, poly-**2**, without humped structure (Figure 7b). This manner of mass transport in the polymer can be supported by the results of Figure 6.

Figure 6 shows that the V_M on the polymer films clearly depended on their structure according to the position (i.e., main or side chain) of the azobenzene group in the polymers. Interestingly, V_M for the main-chain-type polymer, poly-**2** (○), exhibited the largest value among all of the polymers for all irradiation times. Furthermore, the V_M of poly-**2** (○) continuously increased, while that of poly-**1** (□) was saturated after 45 min irradiation. On the other hand, V_M for poly-**3** (△) had a very similar value to that of poly-**1** (□). These results are inconsistent with the values for the efficiency of photoisomerization of the azobenzene moiety in the polymers shown in Figures 2 and 3. Therefore, the results indicate that the total mass transport, V_M, in our polymers is not directly dependent on the softening efficiency of the photoisomerization. In these polymers, V_M may be governed by a mass transport regime related to the incorporation site (i.e., main- and/or side-chain type) of the azobenzene moiety. In other words, poly-**1**, which has the azobenzene moiety in its side chain, was probably more free to deform and could more easily relax back to the initial trans form, which allows the polymer to deform as an incompressible material. Under light irradiation, the molecules of poly-**1** are affected by a scattering force[23] around the spheres, resulting in macroscopic mass transport from the center to the periphery of the structure with little change to the local bulk density ($\Delta\rho_1$) (Figure 7a). On the other hand, poly-**2** has more restricted photoisomerization and a more linear structure than those of the other polymers due to the azobenzene moiety being incorporated in its main chain. These structural features might mean that morphological changes in the polymer could occur more efficiently to decrease the free volume between the polymer chains in the bulk under the light irradiation (Figure 7b). Moreover, morphology changes during the relaxation process may be inhibited by steric hindrance and/or by the rigidity of the main chain. Therefore, it is considered that the change in the local bulk density ($\Delta\rho_2$) around the dents on poly-**2** film is larger than it is on poly-**1**. On the basis of these concepts, the manner of mass transport of poly-**3** can probably also be explained, where interestingly V_M is not intermediate value between poly-**1** and poly-**2** but is similar to that of poly-**1** (Figure 6). Namely, the side chain in poly-**3** restricts the shrinkage of the local bulk due to closer packing of the polymer chains during light irradiation. Thus, the change in the local bulk density ($\Delta\rho_3$) around the dents on the poly-**3** film may be similar to that of poly-**1**, resulting in the formation of a peripheral hump around the structure similar to that seen in poly-**1** (Figure 7c). Consequently, the relationship between the local bulk densities of the polymers can be considered to be roughly as follows:

$$\Delta\rho_2 \gg \Delta\rho_3 \gtrsim \Delta\rho_1 \qquad (3)$$

For further exploration of the mass transport regime in our polymers, we investigated the hardness of the dents by using TMAFM, which showed evidence of the movement of the polymer chains during irradiation. In Figure 8, the TMAFM images show the results for the

same samples as shown in Figure 4a,b. On the side-chain-type polymer (poly-**1**), the phase image shows that the periphery of the dent, corresponding to the humped structural region, became harder (larger phase shift) than the center, as shown in Figure 8a. This result would be clear evidence for the movement of the polymer chains from just below the PS spheres to the periphery. On the other hand, the TMAFM images of the main-chain-type polymer (poly-**2**) very showed that the material inside of the dent as a whole became relatively harder (larger phase shift) than the material outside of the dent (Figure 8b). This also provides evidence for the movement of polymer chains from just below the PS spheres toward the substrate during photoirradiation. These results obviously indicate that the mass transport mechanisms in our polymers are clearly different. It should also be noted from the figure that the depressed region of the dents on the poly-**1** film became softer than the outside of the dents, whereas the equivalent region for poly-**2** became harder. As mentioned in Figure 7, these characteristic probably originate from differences in the migration behavior of the polymer chains for the different polymers, due to the different ways in which the azobenzene moieties are incorporated in the polymers.

Conclusion

To explore the photodeformation behavior of polymers with functional azobenzene moieties in their main and/or side chains, we have investigated the formation of hexagonally arrayed indented structures on thin films of the materials as well as studying their photoisomerization behavior. The indented structures could be formed successfully on the surfaces of the films below their T_g, despite the remarkably slow photoisomerization of the azobenzene moieties in the polymers. Measurements of the depths in the dents were consistent with the dynamics of the azobenzene moiety in the polymers. However, the total amount of mass transport that occurred in the polymers did not depend directly on the efficiency of the photoisomerization process, which might be related to the way that the azobenzene moieties are connected within the polymers. Furthermore, TMAFM image data indicated that the mass transport was induced by two different polymer migration regimes, which are either from the center of the dent toward its periphery or toward the substrate. This study is expected to be useful for the development of superfine photolithography and to optimize the material design for optical data-storage media using azobenzene polymers.

References and Notes

(1) Hvilsted, S.; Andruzzi, F.; Kulinna, C.; Siesler, H. W.; Ramanujam, P. S. *Macromolecules* **1995**, *28*, 2172.
(2) Zilker, S. J.; Bieringer, T.; Haarer, D.; Stein, R. S.; van Egmond, J. W.; Kostromine, S. G. *Adv. Mater.* **1998**, *10*, 855.
(3) Andruzzi, L.; Altomare, A.; Ciardelli, F.; Solaro, R.; Hvilsted, S.; Ramanujam, P. S. *Macromolecules* **1999**, *32*, 448.
(4) Wu, Y.; Kanazawa, A.; Shiono, T.; Ikeda, T.; Zhang, Q. *Polymer* **1999**, *40*, 4787.
(5) (a) Rochon, P.; Gosselin, J.; Natansohn, A.; Xie, S. *Appl. Phys. Lett.* **1992**, *60*, 4. (b) Natansohn, A.; Rochon, P.; Gosselin, J.; Xie, S. *Macromolecules* **1992**, *25*, 2268.
(6) Kumar, J.; Li, L.; Jiang, X.; Kim, D.-Y.; Lee, T. S.; Tripathy, S. K. *Appl. Phys. Lett.* **1998**, *72*, 2096.
(7) Pedersen, T. G.; Johansen, P. M.; Holme, N. C. R.; Ramanujam, P. S.; Hvilsted, S. *Phys. Rev. Lett.* **1998**, *80*, 89.
(8) (a) Sumaru, K.; Yamanaka, T.; Fukuda, T.; Matsuda, H. *Appl. Phys. Lett.* **1999**, *75*, 1878. (b) Sumaru, K.; Fukuda, T.; Kimura, T.; Matsuda, H.; Yamanaka, T. *J. Appl. Phys.* **2002**, *91*, 3421.
(9) Betzig, E.; Trautman, J. K.; Wolfe, R.; Gyorgy, E. M.; Finn, P. L.; Kryder, M. H.; Chang, C.-H. *Appl. Phys. Lett.* **1992**, *61*, 142.
(10) Ohtsu, M.; Hori, H. *Near-Field Nano-Optics*; Kluwer Academic: New York, 1999.
(11) (a) Watanabe, O.; Ikawa, T.; Hasegawa, M.; Tsuchimori, M.; Kawata, Y.; Egami, C.; Sugihara, O. *Mol. Cryst. Liq. Cryst. Sci. Technol., Sect. A* **2000**, *345*, 305. (b) Ikawa, T.; Mitsuoka, T.; Hasegawa, M.; Tsuchimori, M.; Watanabe, O.; Kawata, Y. *J. Phys. Chem. B* **2000**, *104*, *9500*. (c) Ikawa, T.; Hasegawa, M.; Tsuchimori, M.; Watanabe, O.; Kawata, Y.; Egami, C.; Sugihara, O.; Okamoto, N. *Synth. Met.* **2001**, *124*, 159 (d) Watanabe, O.; Ikawa, T.; Hasegawa, M.; Tsuchimori, M.; Kawata, Y. *Appl. Phys. Lett.* **2001**, *79*, 1366. (e) Ikawa, T.; Mitsuoka, T.; Hasegawa, M.; Tsuchimori, M.; Watanabe, O.; Kawata, Y. *Phys. Rev. B* **2001**, *64*, 195408. (f) Hasegawa, M.; Ikawa, T.; Tsuchimori, M.; Watanabe, O.; Kawata, Y. *Macromolecules* **2001**, *34*, 7471.
(12) Xie, S.; Natansohn, A.; Rochon, P. *Chem. Mater.* **1995**, *5*, 403.
(13) Kumar, G. S.; DePra, P.; Neckers, D. C. *Macromolecules* **1984**, *17*, 1912.
(14) Hall, H. K., Jr.; Kuo, T.; Lenz, R. W.; Leslie, T. M. *Macromolecules* **1987**, *20*, 2041.
(15) Tsutsumi, N.; Yoshizaki, S.; Sakai, W.; Kiyo-tsukuri, T. *Macromolecules* **1995**, *28*, 6437.
(16) Lee, T. S.; Kim, D. Y.; Jiang, X. L.; Li, L.; Kumar, J.; Tripathy, S. *Macromol. Chem. Phys.* **1997**, *198*, 2279.
(17) Lee, T. S.; Kim, D.-Y.; Jiang, X. L.; Li, L.; Kumar, J.; Tripathy, S. *J. Polym. Sci., Part A: Polym. Chem.* **1998**, *36*, 283.
(18) Blair, H. S.; Pague, H. I.; Riordan, J. E. *Polymer* **1980**, *21*, 1195.
(19) Heldmann, C.; Warner, M. *Macromolecules* **1998**, *31*, 3519.
(20) Xu, Z.; Drnoyan, V.; Natansohn, A.; Rochon, P. *J. Polym. Sci., Part A: Polym. Chem.* **2000** *38*, 2245.
(21) Bohm, N.; Materny, A.; Keifer, W.; Steins, H.; Muller, M. M.; Schottner, G. *Macromolecules* **1996**, *29*, 2599.
(22) Under the same experimental condition in this study, we confirmed that the $S_0(t)/S_0(0)$ value of a urethane polymer (poly-DR19), bearing DR19-type azobenzene in its side chain, reached a constant within only ~1 min after turning the pump light on. Furthermore, it took less than 1 s for the isomerization (~30%) of the cis form of the azobenzene in poly-DR19 to its trans form after turning the light off.
(23) The force can be induced by absorption of light in dielectric materials and acts parallel with the momentum of the photon.[11e]

MA034122Y